Asian Journal of Agriculture and Biology
https://doi.org/10.35495/ajab.2024.252

Original Article

Immunodetection of highly methyl-esterified pectin in zygotic embryos and solid endosperms of *Cocos nucifera* L.

Aparicio-Ortiz Mónica[1], Juárez-Monroy Dilery[1], Canto-Canché Blondy[2], Tzec-Simá Miguel[1], Islas-Flores Ignacio[1*]
[1]Unidad de Biología Integrativa, Centro de Investigación Científica de Yucatán, A.C., calle 43 No. 130 x 32 y 34, Chuburná de Hidalgo, C.P. 97205, Mérida, Yucatán, México
[2]Unidad de Biotecnología, Centro de Investigación Científica de Yucatán, A.C., calle 43 No. 130 x 32 y 34, Chuburná de Hidalgo, C.P. 97205, Mérida, Yucatán, México

**Corresponding author's email:* islasign@cicy.mx
Received: 28 November 2024 / Accepted: 23 May 2025 / Published Online: 31 May 2025

Abstract

Highly methyl-esterified pectin (HME-P) is typically found in the primary cell walls of young and embryonic plant cells, where it plays a role in regulating differentiation and maturation processes. In this study, the JIM7 monoclonal antibody, which specifically targets HME-P, was utilized to examine tissue sections of coconut zygotic embryos and solid endosperms from the Yucatan green dwarf cultivar at various developmental stages. The expression of the pectin methyl-esterase gene was also assessed using RT-qPCR. The JIM7 antibody revealed the presence of HME-P surrounding the inner cells of immature embryos at the globular and coleoptile stages. As the embryos progressed to intermediate and mature stages, HME-P was found in various cell types, including those of the plumule. In the immature solid endosperm, HME-P was associated with syncytial cells. At the intermediate stage, it was observed in vesicle-like structures and by the mature stage, it surrounded compact cells in a distinct mosaic pattern, near the corrosion cavity. Analysis of the coconut PME gene expression in solid endosperm and zygotic embryos showed peak expression at the immature stage, followed by a decline at the intermediate and mature stages. These findings were consistent with the immunodetection results obtained with the JIM7 antibody in embryos and endosperms. Overall, this study provides novel insights into the coordinated expression of the PME gene and the dynamics of HME-P during the maturation of coconut zygotic embryos and solid endosperms. These findings suggest a potential role for pectin methyl esterification in zygotic embryogenesis in coconut.

Keywords: Endosperm, Coconut, Embryo, Pectin, JIM7, Methyl-esterification

How to cite this article:
Mónica AO, Dilery JM, Blondy CC, Miguel TS and Ignacio IF. Immunodetection of highly methyl-esterified pectin in zygotic embryos and solid endosperms of *Cocos nucifera* L. Asian J. Agric. Biol. 2025: 2024252. DOI: https://doi.org/10.35495/ajab.2024.252

Introduction

The plant cell wall is a complex and dynamic structure composed of carbohydrates such as pectin, cellulose, hemicellulose, and small amounts of carbohydrate-embedded proteins. The dynamics of the cell wall are promoted, at least in part, by chemical modifications of polysaccharides carried out by cell wall-associated enzymes such as polygalacturonases, pectinesterases, hemicellulases, and cellulases, among others (Du et al., 2020).

Pectin is composed of galacturonic acid (GalA), which can be in the form of homogalacturonan polymer (HG; (1,4)-α-D-GalA polymer), rhamnogalacturonan I polymer (RG-I; (1,2) α-D-Rha- (1,4)-α-D-GalA repeated polymer), rhamnogalacturonan II (RG-II; 4.2 kDa polysaccharide complex) and xylogalacturonan (XGA) (Bethke et al., 2016). The HG- polymer is synthesized in the plant's Golgi apparatus, where it is *O*-acetylated at the O-2 or O-3 of GalA residues by acetyl esterase of the CE13 family (Jermendi et al., 2022; Scheller, 2017), and highly methyl esterified-de-esterified at the carboxyl group at C-6 of GalA polymer by pectin methylesterases (PMEs; EC 3.1.1.11) (Dewhirst et al., 2020; Tang et al., 2020). Highly methyl esterified pectin is vesicle-secreted from the Golgi to be deposited in plant primary cell walls, where pectin can be de-esterified *in situ* by pectin methyl esterases (Pelloux et al., 2007; Yu et al., 2022). Additionally, the pectin in the cell wall may be associated with Ca^{2+} (Chandel et al., 2022). Together, these pectin modifications result in cell wall stiffness or loosening, which is essential for cell-to-cell adhesion, cell defense, cell development, and morphogenesis, including the growth and maturation of seeds and endosperm, and embryo bending (Cruz-Valderrama et al., 2018).

The dynamics of high to low pectin methyl esterification and PME gene expression are hypothesized to be key factors in determining cell fate and promoting cell differentiation. In *Brassica napus,* low BnPME gene expression and HME-P levels were observed during early microspore embryogenesis, totipotency, and proliferation stages. Conversely, late developmental stages and cell differentiation were linked to increased BnPME gene expression and pectin methyl de-esterification (Solís et al., 2016). In pro-embryogenic masses (PMEs) of *Quercus suber*, low QsPME gene expression and high methyl-esterified pectin levels were found. As embryogenesis progressed to heart, torpedo, and cotyledon embryo stages, QsPME gene expression gradually rose while methyl-esterified pectin content decreased in the embryo cell walls (Pérez-Pérez et al., 2019).

On the other hand, the monoclonal JIM7 antibody, which immunodetects HME-P signaled the highest level of methyl-esterified pectin at early stages of embryogenesis in somatic or zygotic embryos in banana (*Musa* spp. AAA) (Xu et al., 2011), *Arabidopsis thaliana* (Sala et al., 2013), zygotic embryos of hot pepper *Capsicum chinense* Jacq (Pérez-Pastrana et al., 2018), and castanea, *Castanea mollisima* (Du et al., 2020). In all of these embryos, the high level of HME-P decreases during embryo maturation (Du et al., 2020; Pérez-Pastrana et al., 2018).

Coconut is an ancient monocotyledonous plant species that is highly resistant to the somatic embryogenic strategy. Even when embryogenic success is achieved, *in vitro* shoot differentiation takes a significant amount of time (Verdeil, 2001; Dapeng et al., 2024). To the best of our knowledge, only one study has focused on the behavior of pectin methyl esterification during somatic embryogenesis in coconut (Verdeil, 2001). Contrary to observations in other plants, high levels of low methyl-esterified pectin were immunodetected at earlier stages of somatic embryogenesis in coconut, while HME-P was scarce and the same profile was found along the transition from embryogenic cells to proembryos (Verdeil, 2001).

In the case of coconut seeds, they are highly marketable and economically valuable worldwide (Grass Ramírez et al., 2023). The proteomics of their solid endosperm (Félix et al., 2023) and zygotic embryo (Granados-Alegría et al., 2024), along with transcriptomics (Yousefi et al., 2023), have been investigated at different stages of seed maturation, revealing interesting findings in those areas. However, there is a gap in knowledge regarding the HME-P and the expression of the pectin methyl esterase gene, and their relationship with the maturation of solid endosperm and zygotic embryos.

Due to our interest in the dynamics of methyl esterification of pectin during embryogenesis and embryo maturation, we conducted a study using zygotic embryos and solid endosperms at immature, intermediate, and mature stages from the coconut Yucatan green dwarf cultivar (YGD). We utilized the JIM7 antibody to analyze the levels of HME-P at these various maturation stages. Additionally, the expression of the PME gene was also monitored to

https://doi.org/10.35495/ajab.2024.252

determine the dynamics of pectin methyl esterification during coconut seed maturation. Our findings add new fundamental knowledge to the biology of the species, particularly in the relationship between HME-P and the maturation of solid endosperm and zygotic embryo.

Material and Methods

Coconut fruit harvesting

Yucatan green dwarf coconut fruits at immature, intermediate, and mature stages were collected from plantations in San Crisanto, Yucatan, Mexico (latitude 21°21´7´´N and longitude 89°10´18´´W). The maturity stages of the coconut fruit and embryo were determined following the criteria outlined by Félix et al. (2023). In summary, immature fruits were 6 to 8 months old, intermediate fruits were 9-10 months old, and mature fruits were 11-14 months old.

Extraction of the solid endosperm and zygotic embryo from coconut seeds

Coconut fruits were de-husked and the seeds were cut in half. Sections measuring 1.5 cm of solid endosperm containing the zygotic embryo were then carefully recovered using a sterile cork-borer and placed in sterile glass flasks.

Solid endosperm and embryo tissue fixation

The embryos, which were surrounded by a fine coat of solid endosperm, were washed with double-distilled sterile water. They were then immersed in individual flasks containing a fixing solution made up of 4% paraformaldehyde in PBS buffer with a pH of 7.2 (3 mM KCl, 138 mM NaCl, 8.1 mM Na_2HPO_4, 1.5 mM KH_2PO_4). The flasks were placed in a vacuum chamber where a negative pressure of -10 psi was applied using a vacuum pump (Labconco) and left overnight at room temperature. After being fixed, the tissues were washed three times for 10 min each in PBS buffer at pH 7.2 and at -10 psi. The tissues were then equilibrated at room temperature and -10 psi for 3 h in 10% sucrose dissolved in PBS buffer, followed by 20% sucrose with 3 drops of NEG-50 (Richard-Allan Scientific Neg 50 Frozen Section Medium, Thermo Fisher) for 3 h, and finally in 30% sucrose with 6 drops of NEG-50 overnight at room temperature and -10 psi.

Tissue sectioning, histology and immunohistochemistry

Plastic molds containing a small volume of the NEG-50 solution were incubated at -27 °C for 20 min. Following this, the tissues were embedded in 30% sucrose with 6 drops of NEG-50, placed in the molds, filled with NEG-50 and frozen at -27 °C for 45 min. The plastic molds were then removed and the frozen tissues were fixed for 15 min at -27 °C on cryostat plates. They were subsequently incubated at -80 °C for 10 min before being sectioned in the cryostat (Leica) at -27 °C. Tissue sections of 10 µm were placed on polylysine-treated glass slides and fixed for 5 min at 60 °C.

Fixed tissue slices were incubated for 10 min at room temperature in 50 µL of PBS-T blocking buffer at pH 7.4 containing 5% bovine serum albumin (BSA) and 0.5% Tween-20. After incubation the blocking buffer was removed and the slices were washed with PBS-T buffer containing 1% BSA for 30 min at 4 °C. Next, a 1:7 dilution of JIM7 monoclonal antibody, which detects HME-P (Clausen et al., 2003; Knox et al., 1990), was added and incubated for 1 hour at 4 °C. The slices were then washed three times with 50 µL of PBS-T-1% BSA. Following this, a 1:50 dilution of the Alexa Fluor 488-conjugated secondary antibody goat anti-rat IgG (Invitrogen) was added, and the slices were incubated for 30 min at room temperature. After another three washes with PBS-T-1% BSA, 10 µL of 1% BSA containing 0.6 µM of Nile red and 1.4 mM of DAPI were added to the tissue sections. The sections were then incubated for 10 min in the dark at room temperature. Subsequently, the tissue sections were washed three more times with PBS-T-1% BSA. Finally, a drop of 100% glycerol was added before covering with a slide. The mounted sections were analyzed using a confocal microscope at 488 nm excitation and 555 nm emission wavelengths for Alexa Fluor, 358 nm excitation and 461 nm emission for DAPI, and 549 nm excitation and 461 nm emission for Nile red.

RNA extraction from the solid endosperm and embryo of coconut

The tissues were extracted using a sterile cork borer and placed in sterile RNase-free 2 mL Eppendorf tubes. They were immediately immersed in liquid nitrogen and stored at -80 °C until processing. Total RNA was extracted following the protocol described by Iqbal et al. (2020): 0.08 g of solid endosperm was

mixed with 1.5% polyvinylpyrrolidone 40 (PVP-40) and macerated in a sterile mortar and pestle with liquid nitrogen until a fine powder was obtained. One milliliter (1 mL) of ICRM buffer [0.4 M ammonium thiocyanate, 0.7 M guanidine thiocyanate, 3.3 mL of 3 M sodium acetate (pH 5), 38 mL phenol, 5 mL glycerol, 1% β-mercaptoethanol, diethylpyrocarbonate (DEPC)-treated water, up to 100 mL] was added to the powder and homogenized.

The homogenate was gently agitated for 1 min at room temperature, then incubated on ice for 10 min. After that, 0.2 mL of chloroform was added and gently agitated for another 30 s. The homogenate was then incubated on ice for an additional 10 min before being centrifuged at 13,564 x *g* for 7 min at 4 °C. The supernatant was recovered, and 1 volume of cold 24:1 chloroform/isoamyl alcohol was added. The supernatant was gently agitated then centrifuged at 13,564 x *g*. The upper aqueous phase (400 µL) was transferred to a new RNase-free tube where 600 µL of cold isopropanol was added. The tubes were gently inverted repeatedly before incubating on ice for 7 min. The samples were then centrifuged at 13,564 x *g* and 4 °C; the supernatants were discarded and the RNA pellets were dried at room temperature for 20 min. The RNA was suspended in 30 µL of RNase-free DEPC-treated water by gently pipetting for 2 min and then stored at –80 °C until cDNA synthesis. RNA from embryos was obtained using Trizol reagent according to the manufacturer's instructions (Invitrogen).

RNA quantitation and cDNA synthesis

Residual DNA was removed from RNAs using DNase I, as per the manufacturer´s instructions (Invitrogen). The RNA integrity and purity were assessed through 1% agarose gel electrophoresis and absorbance measurements at 230, 260, and 280 nm, respectively, using a Nanodrop 2000 (Thermo Scientific). For cDNA synthesis, 1 µg of RNA was mixed with 1 µL of 50 µM oligo (dT20) and 1 µL of 10 mM dNTPs. The mixture was incubated at 65 °C for 5 min, followed by a 1-min cooling period on ice. Then 4 µL of "First-Strand 5X" buffer, 1 µL of 0.1 M DTT, 1 µL of RNaseOUT™, and 1 µL of SuperScript™ III RT (200 units/µL) were added. The mixture was incubated at 50 °C for 50 min followed by a 5-min incubation at 85 °C. The synthesized cDNA was quantified using a Nanodrop 2000, as previously described.

Pectin methyl esterase DNA primer design for PCR and qPCR

The pectin methyl esterase CGR2, isoform X1 cDNA from oil palm (*Elaeis guineensis*) [XM_010924925.4] and datil palm (*Phoenix dactylifera*) [XM_008787306.3], were used as queries to search the coconut genome database. A putative pectin methyl esterase (CGR2 ID: CM017875, version CM017875.1, bioproject PRJNA374600) was identified. A pair of primers was developed for the coconut PME coding sequence (Table 1) using the PrimerQuest tool from IDT (https://www.idtdna.com/PrimerQuest/Home/Index). The amplified PCR product was sequenced at the Instituto Potosino de Investigacion Cientifica y Tecnologica A.C. (LANBAMA, IPICYT), Mexico.

RT-qPCR conditions

Briefly, qPCR reactions were conducted in triplicate. Each reaction included 5.0 µL of SYBR Green qPCR supermix buffer (BIORAD), 0.5 µL of forward and reverse primer pair (0.3 mM each) (Table 1), 1.0 µL of cDNA (50 ng/µL), and 8.1 µL of DEPC-treated water. The qPCR conditions were as follows: initial denaturation at 95 °C for 10 min, denaturation at 95 °C for 15 sec, annealing at 63 °C for 30 sec, and amplification at 72 °C for 45 sec for 40 cycles. The $2^{-\Delta\Delta Ct}$ method (Livak and Schmittgen, 2001) was utilized to determine relative gene expression, with actin serving as the reference gene. Data analysis was performed using GraphPad Prism 9.4.1 software.

Results

Morphological characteristics of the solid endosperm and zygotic embryo in coconut fruits at increasing maturity stages (Figure 1) indicate that the solid endosperm is jelly-like and creamy, yet scarce at the immature stage (Figure 1A). It then turns white and increases its compactness and abundance at the intermediate stage (Figure 1B), finally becoming a white-cream color and even more abundant and compact at the mature stage (Figure 1C). On the other hand, zygotic embryos dramatically change in size, shape, and color; from round to conical-shaped at immature stages (Figure 1D) to small and medium-sized cylinders at intermediate stages (Figure 1E), and white to cream-colored and cylindrical-shaped at the mature stage (Figure 1F).

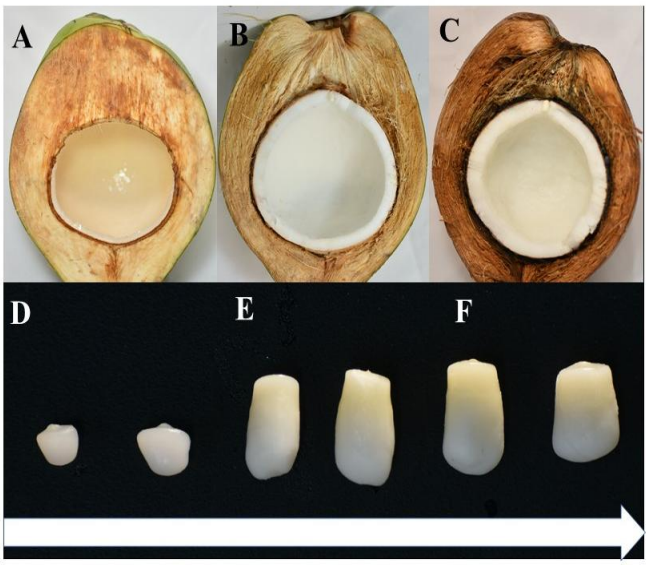

Figure-1. The morphological characteristics of coconut seed solid endosperm and zygotic embryos at various maturation stages.
Panels A and D represent the immature stage, panels B and E represent the intermediate stage, and panels C and F represent the mature stage of solid endosperm and embryos. The arrow indicates the progression of maturation.

Immunodetection of HME-P in coconut zygotic embryos

The JIM7 antibody was used to detect HME-P in coconut embryos at various stages of development: globular-shaped (Figure 2A), coleoptile-conical-shaped (Figure 2F), representing the immature stage, cylinder-shaped (intermediate, Figure 2K), and compact cylinder-shaped (mature embryo, Figure 2P). An abundant, discontinuous signal corresponding to HME-P was observed in the inner medium cells (IMC) and inner basal cells (IBC) of the immature globular embryo. In contrast, a low or no signal was detected in the testa cells (TC) and the suspensor (S) (Figure 2B). It is worth noting that the suspensor was absent in the immature coleoptile-conical-shaped embryo (Figure 2F). HME-P appeared as a bright green web primarily distributed in the internal upper (IUC) or internal medium (IMC) embryo cells, with minimal detection in most external cells (EC) (Figure 2F, G).

The nuclei of cells were stained with 4´,6-diamidino-2-phenylindole (DAPI), which binds to AT-rich regions of double-stranded DNA (Figure 2C, H, M, R) and with Nile red, which binds to polar and neutral lipid-rich environments (Figure 2D, I, N, S). The merging of the different fluorescent signals on the embryo cells revealed that, at the immature globular or coleoptile-conical shaped embryo stages, DAPI and Nile red co-localize in the nuclei of inner upper (IUC) and inner medium (IMC) embryo cells, where pink signals were observed (Figure 2E, J).

Lipids were low or absent at the globular embryo stage, as indicated by the predominant blue signal from DAPI in the nuclei of the inner basal (IBC) and suspensor (S) cells (Figure 2E). In contrast, in the coleoptile-conical embryo, two areas of the inner basal cells (IBC) were filled with lipids, as only the signal of Nile red was observed (Figure 2J).

At the immature coleoptile-conical stage, vesicle-like structures containing HME-P were present in the inner cells of the medium (IMC) and upper part (IUC) of the embryo, but were nearly absent in the basal area (Figure 2G). Signals from DAPI and Nile red were observed in the basal area (Figure 2H, I, J). In the intermediate and mature embryo stages, HME-P was widely distributed in various embryo cells (Figure 2L, O, Q, T), including the plumular leaf (PL) and the embryo endoderm cells (ENC) covering the plumule (P; Figure 2L, Q). However, the intensity of the HME-P signal was lower in the mature embryo (Figure 2Q, T) compared to the intermediate stage, indicating a higher content of HME-P at the intermediate stage. DAPI and Nile red co-localized in some pro-vascular tissues at the plumular leaf (PL) in both intermediate and mature embryos (Figure 2O, T).

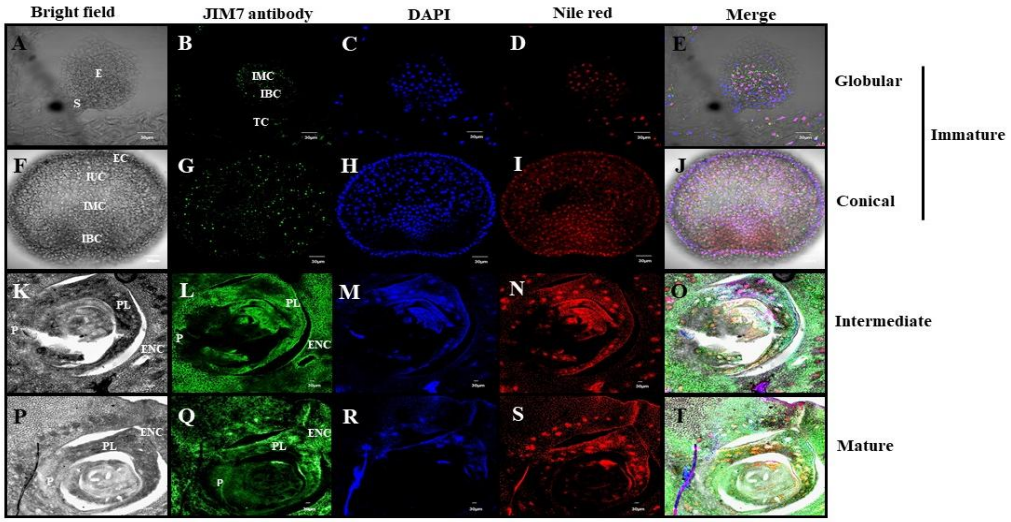

Figure-2. Micrographs of coconut zygotic embryos at various maturity stages.
Panel A displays coconut zygotic embryos at immature (A-E, globular; F-J, conical), intermediate (K-O), and mature (P-T) stages. Panels A, F, K, and P show images from bright field microscopy, while all other images were captured using confocal microscopy. Panels B, G, L, and Q represent HME-P; panels C, H, M and R show DAPI staining for nuclei; panels D, I, N, and S correspond to Nile red staining for lipids. Panels E, J, O, and T display the merged images. In the micrographs, E denotes embryo, S represents suspensor, IUC stands for inner upper cells, IMC for inner medium cells, IBC for inner basal cells, PL for plumular leaf, P for plumule, ENC for endoderm cells, and EC for external cells.

The analysis of solid endosperm cells with the monoclonal antibody JIM7 showed abundant and uniformly distributed methyl-esterified pectin near the testa cell layer (EndCloTes) in a web-like structure covering the syncytium-like cells of immature solid endosperm (Figure 3B) and surrounding the nuclei (Figure 3E). At the intermediate stage, the HME-P was observed in the inner cells of the endosperm (ICEnd) within small, medium and large-sized vesicle-like structures (Figure 3G, J), while in the cells of the mature endosperm close to the corrosion cavity (EndCloCC), most of the JIM7 signal was observed in the cell wall surrounding these endosperm cells (Figure 3L, O). Meanwhile, DAPI and Nile red stained immature endosperm cells located near the testa cell layer (EndCloTes) (Figure 3C, D) and at the internal cells of the endosperm (ICEnd). At the intermediate stage, only a few DAPI and Nile red signals were observed (Figures 3H, I). Similar results were observed in the mature endosperm cells near the corrosion cavity (CC) (Figure 3M, N).

RNA was isolated from immature, intermediate and mature stages of solid endosperms (Figure S1, A) and zygotic embryos (Figure S1, B). Using the endpoint PCR primer pair annotated in Table 1, a 205 bp fragment of the coconut pectin methyl esterase was RT-amplified from RNA isolated from solid endosperms (Figure S1, C). Sequencing of this PCR-amplified fragment confirmed 100% identity and an e-value of 3e-147 with the *C. nucifera* L. Hainan tall pectin methyl esterase CGR2 (Figure S2).

The qPCR primer pair described in Table 1 was used to determine that the PME gene is differentially expressed in solid endosperms and zygotic embryos at different stages of maturity (Figure 4).

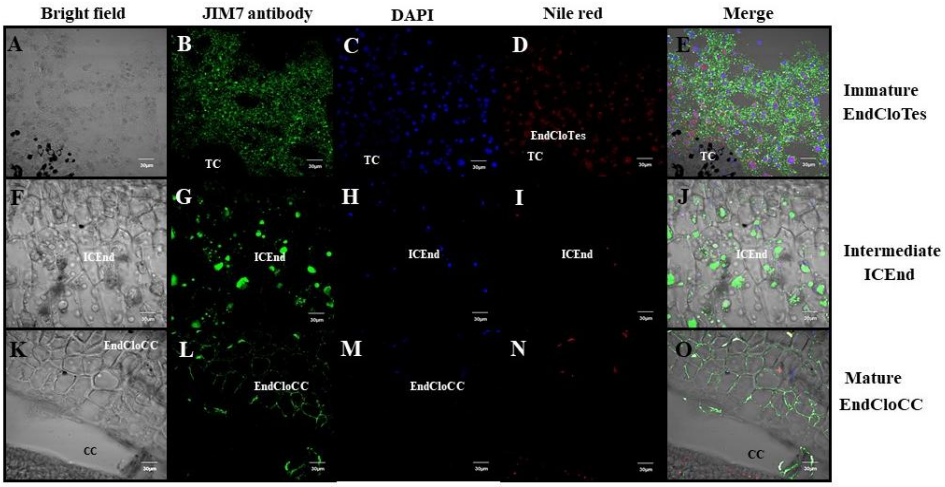

Figure-3. Micrographs of coconut solid endosperm cells at immature, intermediate, and mature stages**.**
The coconut cells of solid endosperms are depicted at immature stages (A-E), intermediate stages (F-J), and mature stages (K-O). Panels A, F, and K display images from bright-field microscopy, while all other images were taken using confocal microscopy. Panels B, G, and L show JIM7 antibody detection; panels C, H, and M show the nuclei stained with DAPI; panels D, I, and N show lipids stained with Nile red; and panels E, J, and O show the merged images. TC= Testa cells, EndCloTes= Immature endosperm close to the testa, ICEnd= Intermediate cells of endosperm, EndHaus= Intermediate endosperm of haustorium, EndCloHau= Mature endosperm close to the haustorium, CC= corrosion cavity.

Table-1. Target genes, oligonucleotide-designed primers, and the length of the resulting PCR products. Base pair (bp).

Target Gene	Primer Nucleotide Sequence	PCR product length (bp)
Consensus nucleotide sequences of pectin methyl esterases from *Elaies guineensis* (XM_010924925.4) and *Phoenix dactylifera* (XM_008787306.3)	F-5′-GAACCTTATGACTTGGAGGATGT-3′ R-5′CCAGCAAATATAACAAGACCATCTG-3′	221
		qPCR
Putative pectin methyl esterase gene from *Cocos nucifera* L. CGR2, ID: CM017875, version CM017875.1, bioproject PRJNA374600	F-5′-AAAGGCTTTGTCCGTTTAGC-3′ R-5′-GATGAATAAAGATGCCAAAGAACTG-3′	205
		qPCR
Actin from *Cocos nucifera* L. CM017876.1	F-5′-TGGTATCCACGAGACCACCT-3′ R-5′-TCATACGGTCACCAATGCCC-3′	125

The highest expression was observed at the immature stage in the zygotic embryo and solid endosperm, with an average fold change close to 1.2 and 1.4, respectively. This was followed by 1.05 and 0.79 at the intermediate and mature embryo stages, respectively. In solid endosperm, the average fold changes were 0.82 and 0.92 at the intermediate and mature stages, respectively (Figure 4). Tukey´s statistical analysis indicated that at the immature and intermediate stages in embryos, PME gene expression was similar but statistically different from the mature embryo stage. On the other hand, Tukey´s analysis showed that at the immature stage, the PME gene expression is statistically different from the intermediate and mature stages, but there are no differences between the last two endosperm stages.

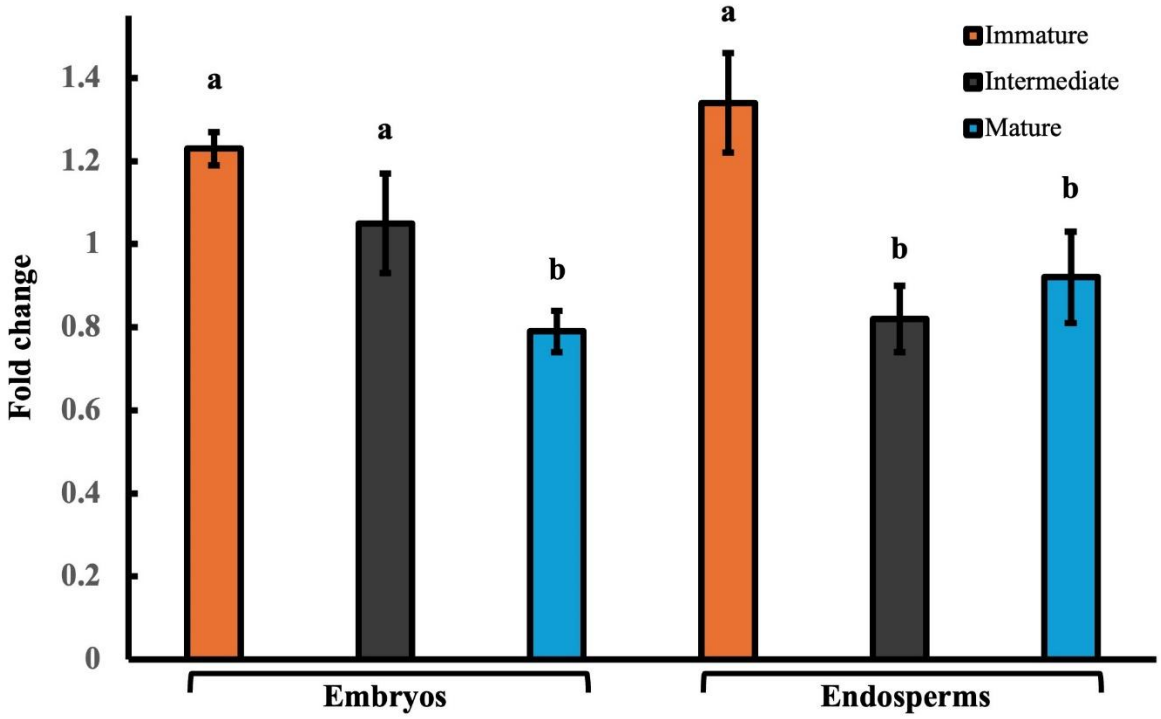

Figure-4. The relative expression of the pectin methyl esterase gene in coconut zygotic embryos and solid endosperms at three maturity stages.
The actin gene was used as a reference. The relative expression of the pectin methyl esterase gene was compared to the endogenous actin gene expression. Tukey´s statistical analysis was; conducted at a significance level of 0.05. If the vowels in the figure are the same, there are no statistical differences; if the vowels are different, it means there are statistical differences.

Discussion

Plant cell wall dynamics play a crucial role in processes such as embryogenesis, cell differentiation, growth and seed maturation (Levesque-Tremblay et al., 2015). The hardness of coconut seed tissues and embryo increases as they mature (Figure 1) (Félix et al., 2023; Granados-Alegría et al., 2024). However, many of the biochemical and molecular events that occur during seed maturation, such as the expression of the pectin methyl esterase gene and HME-P, have not been analyzed yet.

Results from the Yucatan green dwarf coconut cultivar seed showed that embryo differentiation begins five to six months after pollination. Initially, the embryo remained arrested as a few cells. Division and differentiation of the embryo started at six to seven months, simultaneously with the deposition of the solid endosperm on the inner face of testa cells (Figure 1). Maturation of the solid endosperm and embryo occurs between eight and fourteen months after pollination. Our findings are consistent with those of Angeles et al. (2018), who stated that coconut seed development and maturation take 12-14 months after pollination, depending on the variety. They also noted

that in the Makapuno and Lono cultivars, differentiation and accumulation of the solid endosperm begin six months after pollination.

In monocot seeds, as zygotic globular embryos transition into the coleoptile shape, cells show high proliferative activity, increasing in both number and volume. This process leads to the development of the embryonary cotyledon, dermal outer and inner cells, as well as root and apical meristems (De Vries and Weijers, 2017; Du et al., 2020; Juarez-Escobar et al., 2021). This provides an opportunity to investigate the potential connection between cell differentiation and HME-P dynamics.

In the case of the YGD coconut seed, immunodetection with the JIM7 antibody showed the presence of HME-P in embryos and solid endosperms. The complexity and distribution of HME-P increased from the immature to the mature stage (Figures 2, 3). Our results contradict Verdeil (2001), who observed a more intense signal of gold-JIM5 (which detects non- or scarce methyl esterified pectin) than the JIM7 antibody in the primary walls of cells transitioning from embryogenic tissues to somatic proembryos in coconut. Unfortunately, the significance of these findings was not elaborated upon in their study. The strong signal of JIM5 found in their study likely indicated cells undergoing remodeling of their primary cell walls, especially as the primary and secondary cell walls became more elastic. During this process, the high content of low methyl-esterified pectin likely transformed into a high content of HME-P in cells that were gaining embryogenic competence and forming proembryos. Similar findings were reported in the monocot *Musa* spp. AAA (Xu et al., 2011).

In the development of zygotic embryos and solid endosperms of coconuts, JIM7 decorated all the growing cells because they had newly synthesized cell walls with HME-P, promoting cell wall flexibility for growth. Our results align with the findings of Levesque-Tremblay et al. (2015), who suggested that HME-P in *A. thaliana* seeds is a result of the enzymatic activity of methyl esterase. This activity is necessary for loosening the cell wall in the embryo to facilitate cell expansion and the accumulation of storage reserves. Furthermore, the distribution of the strong JIM7 signal in coconut embryos resembled that described in the different tissues of *C. mollissima* and *Arabidopsis thaliana* embryos (Cruz-Valderrama et al., 2018). This indicates a temporal-spatial regulation of pectin methyl esterification during the maturation of plant zygotic embryo.

Once the coconut endosperm covers the globular embryo, the endosperm is rapidly remodeled around the growing, differentiating, and expanding embryo, and then both initiate their maturation. In the immature endosperm, the JIM7 antibody decorated the cell walls of the syncytium cells, which at this stage showed large nuclei (Figure 3B, E). Some of these nuclei stained blue, as expected, while others stained pink (Figure 3C, E), suggesting an association with oils or hydrophobic compounds. At the intermediate stage of the endosperm, in addition to cell wall staining, a strong JIM7 signal was associated with vesicle-like structures (Figure 3G, J), suggesting that HME-P is secreted or transported to the endosperm cell walls through vesicles, as previously suggested by Yu et al. (2022). Our findings of HME-P in coconut endosperm syncytial cells revealed the presence of cell walls in these cells, in disagreement with the previous proposal from Angeles et al. (2021), stating that syncytial cells lack cell walls. In the case of *A. thaliana*, a species whose embryos bend in the endosperm, the JIM7 bound heterogeneously to the cell walls of the endosperm containing bending embryos at torpedo and mature stages (Ali et al., 2023; Cruz-Valderrama et al., 2018); however, coconut embryos did not show bending during maturation.

In the mature endosperm, JIM7 was found to be associated with the cell walls of cells located beneath the first layer of cells that are in contact with the corrosion cavity (Figure 3L; EndCloCC). Further into the tissue, JIM7 was observed to strongly decorate endosperm cell walls and a few vesicle-like structures (Figure 3L, O). These findings align with a previous study that demonstrated HME-P is produced in the Golgi apparatus and then transported in vesicles to the cell walls (Yu et al., 2022).

Together, the results in scientific reports regarding HME-P in different plant zygotic embryos along with our findings in coconut zygotic embryos, support the idea that pectin methyl esterification is a conserved metabolic event that plays a key role during the growth and maturation of plant embryos. Due to the conservation of HME-P, it could be utilized as a biochemical marker to select plant material with high cell totipotency for introduction into *in vitro* biotechnological processes such as plant micropropagation, or embryo rescue and preservation, which are current bottlenecks in coconut production (Nikila et al., 2025).

On the other hand, extracting ribonucleic acid (RNA) from coconuts, specifically from solid endosperm and

embryos, has proven to be a challenging task due to the presence of polysaccharides, proteins, polyphenols and lipids that bind to the RNA (Iqbal et al., 2020; Nguyen and Vu, 2023). We successfully isolated RNA from the solid endosperm and zygotic embryo (Figure S1) and performed RT-PCR, which amplified a 205 bp DNA product corresponding to a fragment of a coconut PME esterase transcript (Figure S2). To the best of our knowledge, this is the first analysis of PME gene expression in coconus.

The expression of the pectin methyl esterase gene was highest in the immature and intermediate stages of the zygotic embryos, with a further decrease at the mature stage. Similarly, in the solid endosperms, the highest PME gene expression occurred at the immature stage, decreasing to similar levels at the intermediate and mature stages (Figure 4).

Results from PME gene expression in coconut zygotic embryos are consistent with findings in *A. thaliana*, where the pectin methyl esterase gene was highly expressed early during seed maturation. Cases where mutation of the PME gene in *A. thaliana* causes embryo malformation support the idea that this enzyme is key for embryo development and maturation (Levesque-Tremblay et al., 2015; Wolf et al., 2009). During the induction of somatic embryogenesis in the cork oak (*Quercus suber* L.), low gene expression of the QsPME gene was detected at the pro-embryogenic masses. It then increased at the heart-torpedo stage, reaching the highest gene expression at mature cotyledon embryos (Pérez-Pérez et al., 2019). Consequently, the expression of the pectin methyl esterase gene and the methyl esterification of pectin are common occurrences in plant somatic and zygotic embryogenesis. However, overall, the results suggest that specific differences exist in the PME gene expression and methyl esterification of pectin among different plant species. The expression of the PME gene in coconut is consistent with the highest JIM7 antibody signal observed at immature and intermediate stages of zygotic embryos and solid endosperm, in comparison with the mature stage of both tissues (Figures 2, 3).

Conclusion

Some of the cell differentiation occurring during coconut zygotic embryo and endosperm maturation is related to HME-P dynamics in their cell walls. Differences in HME-P during zygotic embryo and endosperm maturation were revealed by immunodetection with the JIM7 antibody and by qRT-PCR assays evaluating the expression levels of the methyl esterase gene. The JIM7 antibody showed differences in pectin methyl esterification between the zygotic embryo and endosperm; an organized web-like structure was observed in the immature embryo, while an abundant signal was observed in all syncytial cells in the immature endosperm. At mature stages of embryo and endosperm, HME-P accumulation decreased. In coconut, future research on the importance of the dynamics of methyl esterification of pectin should focus on functional characterization of the cloned gene using gene knock-out, gene silencing or CRISPR-Cas methodologies. Another possibility is using changes in methyl esterification of pectin as a biochemical marker to select plant tissues with high embryogenic totipotency to improve *in vitro* coconut plant regeneration.

Acknowledgments

The authors would like to thank CONAHCYT for funding the project CB-2017-2018-A1-S-10398 and the scholarships 776663 and 774862 granted to M. Aparicio-Ortiz and D. Juárez-Monroy, for their Master Sciences studies; special thanks to M. Sc. Jewel Nicole Anna Tod for their critical reading and language revision of the manuscript.

Disclaimer: None.

Conflict of Interest: None.

Source of Funding: Consejo Nacional de Humanidades Ciencia y Tecnologias (CONAHCYT) provide economical support to the project CB-2017-2018-A1-S-10398

Contribution of Authors

Ignacio IF: Wrote and reviewed the manuscript and coordinated the experimental work.

Blondy CC: Wrote and reviewed the manuscript.

Mónica AO, Dilery JM & T Miguel TS: Carried out the experimental work and processed the data.

References

Ali MF, Shin JM, Fatema U, Kurihara D, Berger F, Yuan L and Kawashima T, 2023. Cellular dynamics of coenocytic endosperm development in *Arabidopsis thaliana*. Nat. Plants 9(2): 330–342. https://doi.org/10.1038/s41477-022-01331-7.

Angeles J, Lado J, Pascual E, Cueto C, Laurena A and Laude R, 2018. Towards the Understanding of Important Coconut Endosperm Phenotypes: Is there an Epigenetic Control? Agronomy 8(10): 225. https://doi.org/10.3390/agronomy8100225.

Angeles JGC, Lado JP, Pascual ED, Laurena AC and Laude RP, 2021. Epigenetic Considerations on Altered Phenotypes of the Coconut Endosperm, pp. 175-190. In M.K. Rajesh, S.V. Ramesh, L. Perera, and C. Kole (eds.), The Coconut Genome, Compendium of Plant Genomes. Springer International Publishing, Switzerland. https://doi.org/10.1007/978-3-030-76649-8_13.

Bethke G, Thao A, Xiong G, Li B, Soltis NE, Hatsugai N, Hillmer RA, Katagiri F, Kliebenstein DJ, Pauly M and Glazebrook J, 2016. Pectin Biosynthesis Is Critical for Cell Wall Integrity and Immunity in *Arabidopsis thaliana*. Plant Cell. 28(2): 537–556. https://doi.org/10.1105/tpc.15.00404.

Chandel V, Biswas D, Roy S, Vaidya D, Verma A and Gupta A, 2022. Current Advancements in Pectin: Extraction, Properties and Multifunctional Applications. Foods. 11(17): 2683. https://doi.org/10.3390/foods11172683.

Clausen MH, Willats WGT and Knox JP, 2003. Synthetic methyl hexagalacturonate hapten inhibitors of anti-homogalacturonan monoclonal antibodies LM7, JIM5 and JIM7. Carbohydr. Res. 338(17): 1797–1800. https://doi.org/10.1016/S0008-6215(03)00272-6.

Cruz-Valderrama JE, Jiménez-Durán K, Zúñiga-Sánchez E, Salazar-Iribe A, Márquez-Guzmán J and Gamboa-de Buen A, 2018. Degree of pectin methyl esterification in endosperm cell walls is involved in embryo bending in *Arabidopsis thaliana*. Biochem. Biophys. Res. Commun. 495(1): 639–645. https://doi.org/10.1016/j.bbrc.2017.11.077.

Dapeng Z, Zhiying L, Yin Min H, Peng S, Xueke W, Hao N, Jingjing N, Lihuan W, Faiza-Shafique K, Qun Y, Saira B and Yong W, 2024. Insights into the developmental trajectories of zygotic embryo, embryogenic callus and somatic embryo in coconut by single-cell transcriptomic analysis. Ind. Crops Prod. 212: 118338. https://doi.org/10.1016/j.indcrop.2024.118338.

De Vries SC and Weijers D, 2017. Plant embryogenesis. Curr. Biol. 27(17): R870–R873. https://doi.org/10.1016/j.cub.2017.05.026.

Dewhirst RA, Afseth CA, Castanha C, Mortimer JC and Jardine KJ, 2020. Cell wall O-acetyl and methyl esterification patterns of leaves reflected in atmospheric emission signatures of acetic acid and methanol. PLoS One. 15(5): e0227591. https://doi.org/10.1371/journal.pone.0227591

Du B, Zhang Q, Cao Q, Xing Y, Qin L and Fang K, 2020. Changes of cell wall components during embryogenesis of *Castanea mollissima*. J. Plant Res. 133: 257–270. https://doi.org/10.1007/s10265-020-01170-7.

Félix JW, Granados-Alegría MI, Gómez-Tah R, Tzec-Simá M, Ruíz-May E, Canto-Canché B, Zamora-Briseño JA, Bojórquez-Velázquez E, Oropeza-Salín C and Islas-Flores I, 2023. Proteome Landscape during Ripening of Solid Endosperm from Two Different Coconut Cultivars Reveals Contrasting Carbohydrate and Fatty Acid Metabolic Pathway Modulation. Int. J. Mol. Sci. 24(13): 10431. https://doi.org/10.3390/ijms241310431.

Granados-Alegría MI, Canto-Canché B, Gómez-Tah R, Félix JW, Tzec-Simá M, Ruiz-May E and Islas-Flores I, 2024. Proteomic Profiling of *Cocos nucifera* L. Zygotic Embryos during Maturation of Dwarf and Tall Cultivars: The Dynamics of Carbohydrate and Fatty Acid Metabolism. Int. J. Mol. Sci. 25(15): 8507. https://doi.org/10.3390/ijms25158507.

Grass Ramírez JF, Muñoz RC and Zartha Sossa JW, 2023. Innovations and trends in the coconut agroindustry supply chain: A technological surveillance and foresight analysis. Front. Sustain. Food Syst. 7: 1048450. https://doi.org/10.3389/fsufs.2023.1048450.

Iqbal A, Yang Y, Wu Y, Li J, Hamayun M, Hussain A and Shah F, 2020. An easy and robust method for the isolation of high quality RNA from coconut tissues. Electron. J. Biotechnol. 48: 78–85. https://doi.org/10.1016/j.ejbt.2020.09.008.

Jermendi É, Beukema M, van den Berg MA, de Vos P and Schols HA, 2022. Revealing methyl-esterification patterns of pectins by enzymatic fingerprinting: Beyond the degree of blockiness. Carbohydr. Polym. 277:118813. https://doi.org/10.1016/j.carbpol.2021.118813.

Juarez-Escobar J, Bojórquez-Velázquez E, Elizalde-Contreras JM, Guerrero-Analco JA, Loyola-Vargas VM, Mata-Rosas M and Ruiz-May E, 2021. Current Proteomic and Metabolomic Knowledge of Zygotic and Somatic Embryogenesis in Plants. Int. J. Mol. Sci. 22(21): 11807. https://doi.org/10.3390/ijms222111807.

Knox JP, Linstead PJ, King J, Cooper C and Roberts K, 1990. Pectin esterification is spatially regulated both within cell walls and between developing tissues of root apices. Planta 181(4): 512–521. https://doi.org/10.1007/BF00193004.

Levesque-Tremblay G, Müller K, Mansfield SD and Haughn GW, 2015. HIGHLY METHYL ESTERIFIED SEEDS Is a Pectin Methyl Esterase Involved in Embryo Development. Plant Physiol. 167(3): 725–737. https://doi.org/10.1104/pp.114.255604.

Livak KJ and Schmittgen TD, 2001. Analysis of Relative Gene Expression Data Using Real-Time Quantitative PCR and the 2−ΔΔCT Method. Methods. 25(4): 402–408. https://doi.org/10.1006/meth.2001.1262.

Nguyen TD and Vu HT, 2023. Evaluation of Methods for Total RNA Extraction from the endosperm of *Cocos nucifera* var. makapuno in Vietnam for Molecular Analysis. Biotropia 30(3): 384–395. https://doi.org/10.11598/btb.2023.30.3.2027.

Nikila A, Renuka R, Kumar KK, Mohanalakshmi M, Suresh J and Thavaprakash N, 2025. Advances in coconut micropropagation: prospects, constraints and way forward. Plant Sci. Today 12(sp1): 01-13. https://doi.org/10.14719/pst.5826.

Pelloux J, Rusterucci C and Mellerowicz E, 2007. New insights into pectin methylesterase structure and function. Trends Plant Sci. 12(6): 267–277. https://doi.org/10.1016/j.tplants.2007.04.001.

Pérez-Pastrana J, Islas-Flores I, Bárány I, Álvarez-López D, Canto-Flick A, Canto-Canché B, Peña-Yam L, Muñoz-Ramírez L, Avilés-Viñas S, Testillano PS and Santana-Buzzy N, 2018. Development of the ovule and seed of Habanero chili pepper (*Capsicum chinense* Jacq.): Anatomical characterization and immunocytochemical patterns of pectin methyl-esterification. J. Plant Physiol. 230: 1–12. https://doi.org/10.1016/j.jplph.2018.08.005.

Pérez-Pérez Y, Carnero E, Berenguer E, Solís MT, Bárány I, Pintos B, Gómez-Garay A, Risueño MC and Testillano PS, 2019. Pectin De-methylesterification and AGP Increase Promote Cell Wall Remodeling and Are Required During Somatic Embryogenesis of *Quercus suber*. Front. Plant Sci. 9: 1915. https://doi.org/10.3389/fpls.2018.01915.

Sala K, Potocka I and Kurczynska E, 2013. Spatio-temporal distribution and methyl-esterification of pectic epitopes provide evidence of developmental regulation of pectins during somatic embryogenesis in *Arabidopsis thaliana*. Biol. Plant. 57(3): 410–416. https://doi.org/10.1007/s10535-013-0304-6.

Scheller HV, 2017. Plant cell wall: Never too much acetate. Nat Plants. 3(3): 17024. https://doi.org/10.1038/nplants.2017.24.

Solís MT, Berenguer E, Risueño MC and Testillano PS, 2016. BnPME is progressively induced after microspore reprogramming to embryogenesis, correlating with pectin de-esterification and cell differentiation in *Brassica napus*. BMC Plant Biol. 16(1): 176. https://doi.org/10.1186/s12870-016-0863-8.

Tang C, Zhu X, Qiao X, Gao H, Li Q, Wang P, Wu J and Zhang S, 2020. Characterization of the pectin methyl-esterase gene family and its function in controlling pollen tube growth in pear (*Pyrus bretschneideri*). Genomics 112: 2467–2477. https://doi.org/10.1016/j.ygeno.2020.01.021.

Verdeil J, 2001. Ultrastructural Changes in Coconut Calli Associated with the Acquisition of

Embryogenic Competence. Ann. Bot. 88(1): 9–18. https://doi.org/10.1006/anbo.2001.1408.

Wolf S, Mouille G and Pelloux J, 2009. Homogalacturonan Methyl-Esterification and Plant Development. Mol. Plant. 2(5): 851–860. https://doi.org/10.1093/mp/ssp066.

Xu C, Zhao L, Pan X and Šamaj J, 2011. Developmental Localization and Methylesterification of Pectin Epitopes during Somatic Embryogenesis of Banana (*Musa* spp. AAA). PLoS One. 6(8): e22992. https://doi.org/10.1371/journal.pone.0022992

Yousefi K, Abdullah SNA, Hatta MAM and Ling KL, 2023. Genomics and Transcriptomics Reveal Genetic Contribution to Population Diversity and Specific Traits in Coconut. Plants (Besel). 12(9): 1913. https://doi.org/10.3390/plants12091913.

Yu Y, Cui L, Liu X, Wang Y, Song C, Pak U, Mayo KH, Sun L and Zhou Y, 2022. Determining Methyl-Esterification Patterns in Plant-Derived Homogalacturonan Pectins. Front. Nutr. 9: 925050. https://doi.org/10.3389/fnut.2022.925050.

Supplementary Material

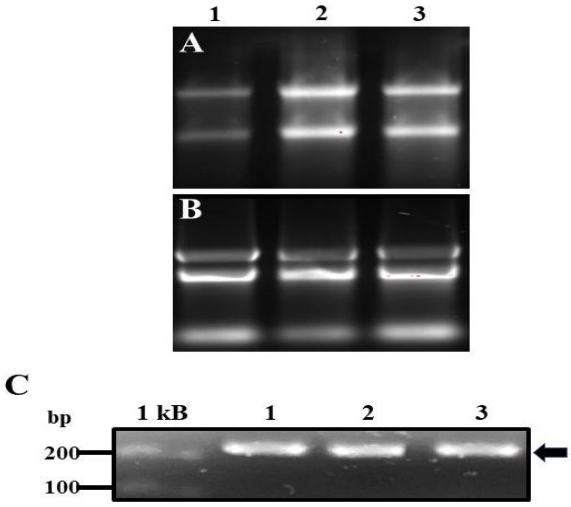

Figure-S1. RNA isolated from coconut solid endosperms and zygotic embryos at different maturity stages and specific PCR amplification of a fragment of the pectin methyl esterase transcript.
RNA extracted from solid endosperms (A) and zygotic embryos (B). An RT-PCR fragment of 205 bp (C) was amplified using specific primers for the pectin methyl esterase transcript at immature (1), intermediate (2), and mature (3), stages. A 1 kB DNA ladder (Invitrogen) was used for size reference.

```
aaaggctttgtccgtttagctgatatcaagtttcctctcctgccatacaggccaaaatca
 K  G  F  V  R  L  A  D  I  K  F  P  L  L  P  Y  R  P  K  S
ttttccctcgtcatagtttcagatgcactggactacttatctccaaagtatctcaacaag
 F  S  L  V  I  V  S  D  A  L  D  Y  L  S  P  K  Y  L  N  K
acccttccagatttggcaagggtatcctcagatggtcttgttatatttgctggtagtatt
 T  L  P  D  L  A  R  V  S  S  D  G  L  V  I  F  A  G  S  I
cagttctttggcatctttattcatc
 Q  F  F  G  I  F  I  H
```

Figure-S2. The nucleotide sequence of the cDNA fragment (205 bp) amplified from coconut solid endosperm and embryos.
Lowercase letters indicate the nucleotide sequence, while capital letters correspond to the *in-silico*-deduced sequence of amino acids.

https://doi.org/10.35495/ajab.2024.252